Soft-gluon effects in WW production at hadron colliders

Massimiliano Grazzini

INFN, Sezione di Firenze and
Dipartimento di Fisica, Università di Firenze
I-50019 Sesto Fiorentino, Florence, Italy
E-mail: `massimiliano.grazzini@cern.ch`

ABSTRACT: We consider QCD radiative corrections to WW pair production in hadron collisions. We perform a calculation that consistently combines next-to-leading order predictions with soft-gluon resummation valid at small transverse momenta p_T^{WW} of the WW pair. We present results for the p_T^{WW} distribution at the LHC up to (almost) next-to-next-to-leading logarithmic accuracy, and study the effect of resummation on the charged-lepton distributions. Soft-gluon effects are typically mild, but they can be strongly enhanced when hard cuts are applied. The relevant distributions are generally well described by the MC@NLO event generator.

Contents

1. Introduction

Vector boson pair production in hadron collisions is important for physics within and beyond the Standard Model (SM). First of all, this process can be used to measure the vector boson trilinear couplings. Any deviation from the pattern predicted by SU(2) ⊗ U(1) gauge invariance would be a signal of new physics. The Tevatron collaborations are currently measuring WW, WZ and $W\gamma$ cross sections at invariant masses larger than those probed at LEP2, setting limits on the corresponding anomalous couplings [1].

Furthermore, vector boson pairs are an important background for new physics searches. If a heavy enough Higgs boson does exist, it will decay with large branching ratios in WW and ZZ pairs, whereas charged Higgs bosons from non standard Higgs sectors may decay into WZ final states [2]. Typical signals of supersymmetry, e.g. three charged leptons plus missing energy, find an important background in WZ and $W\gamma$ production [3].

In this context, WW production has received considerable attention. This process provides an irreducible background to the Higgs boson search in the $H \rightarrow WW \rightarrow l\nu l\nu$ channel, which is the most important when the mass M_H of the Higgs boson is in the range $155 \lesssim M_H \lesssim 170\,\text{GeV}$. Since two neutrinos are present in the final state, no invariant-mass peak can be reconstructed. Fortunately, the angular correlations among the charged leptons suggest a good discrimination of the signal over the background [4], provided the background can be reliably extrapolated into the signal region. It is thus essential to have good control on the SM prediction for the WW cross section as well as for the associated distributions.

QCD corrections to WW production at next-to-leading-order (NLO) have been computed more than 10 years ago [5, 6] and enhance the cross section by about 40% at LHC energies. These calculations were done with the traditional method of evaluating directly the relevant squared amplitudes. As a consequence, the W's polarization was summed over and spin correlations were not taken into account.

More recent NLO calculations exist that, using the one-loop helicity amplitudes computed in ref. [7], fully take into account spin correlations [8]. The general purpose NLO

program MCFM [9] includes in addition single-resonant contributions neglected in the calculation of ref. [8]. Very recently, the effect of the potentially large next-to-next-to-leading (NNLO) contribution from the one-loop $gg \to WW \to l\nu l\nu$ diagrams has also been studied [10, 11].

The fixed-order NLO calculations provide a reliable estimate of WW cross sections and distributions as long as the scales involved in the process are all of the same order. When the transverse momentum of the WW pair p_T^{WW} is much smaller than its invariant mass M_{WW} the validity of the fixed-order expansion may be spoiled since the coefficients of the perturbative expansion can be enhanced by powers of the large logarithmic terms, $\ln^n M_{WW}/p_T^{WW}$. This is certainly the case for the p_T^{WW} spectrum, which, when evaluated at fixed order, is even divergent as $p_T^{WW} \to 0$, and thus requires an all-order resummation of the logarithmically enhanced terms. Resummation effects, however, can be visible also in other observables, making it important to study them in detail.

The way to perform transverse-momentum resummation is known [12]–[20]: to correctly implement momentum conservation in the transverse plane the resummation has to be performed in impact parameter b-space, b being the variable conjugated to p_T through a Fourier transformation. In the case of vector boson pair production, transverse-momentum resummation has been applied to $\gamma\gamma$ [21] and ZZ [22] pair production. To our knowledge, the case of WW pair production has not been considered yet.

In the present paper we report on an implementation of b-space resummation to WW production in hadron collisions. We use the helicity amplitudes of ref. [7] and work in the narrow width approximation (i.e. we only consider double-resonant contributions), but fully include the decay of the W's, keeping track of their polarization in the leptonic decay. In the large p_T^{WW} region we use LO perturbation theory (WW+1 parton); in the region $p_T^{WW} \ll M_{WW}$ the large logarithmic contributions are resummed to (almost) next-to-next-to-leading logarithmic (NNLL) [23, 24] accuracy. Our results have thus uniform NLO accuracy but consistently include the effect of resummation in the region $p_T^{WW} \ll M_{WW}$.

To perform the resummation we use the formalism of refs. [25, 26]. In this approach, the resummation is achieved at the level of the partonic cross section and the large logarithmic contributions are exponentiated in a process-independent manner, being constrained to give vanishing contribution to the total cross section.

Besides computing transverse momentum spectra of the WW pair, we study the effect of resummation on the leptonic distributions, when different cuts are applied. We also compare our results with those obtained at NLO and with the ones from the general purpose event generator MC@NLO [27], which, in its latest release [28], partially includes the effect of spin correlations in the W's decay.

The paper is organized as follows. In section 2 we discuss the application of b-space resummation to WW production. In section 3 we present our numerical results and in section 4 we draw our conclusions.

Preliminary results of this work for the p_T^{WW} spectrum were used in the study of ref. [29].

2. Transverse-momentum resummation for WW pair production

In this section we apply b-space resummation to the production of WW pairs in hadron collisions. The resummation formalism we use is completely general, and, as discussed in detail in ref. [26], can be applied to a generic process in which a system of non strongly interacting particles of high mass M is produced in hadronic collisions. In the case of WW production, the mass M is the invariant mass of the WW system.

The resummation is performed at the level of the partonic cross section, which is decomposed as:

$$\frac{d\hat{\sigma}_{WW\,ab}}{dM^2 dp_T^2} = \frac{d\hat{\sigma}_{WW\,ab}^{(\text{res.})}}{dM^2 dp_T^2} + \frac{d\hat{\sigma}_{WW\,ab}^{(\text{fin.})}}{dM^2 dp_T^2}. \tag{2.1}$$

The first term on the right hand side, $d\hat{\sigma}_{WW\,ab}^{(\text{res.})}$, contains all the logarithmically enhanced contributions at small p_T, and has to be evaluated by resumming them to all orders in α_S. The second term, $d\hat{\sigma}_{WW\,ab}^{(\text{fin.})}$, is free of such contributions, and can thus be evaluated at fixed order in perturbation theory.

The resummed component $d\hat{\sigma}_{WW\,ab}^{(\text{res.})}$ can be expressed as

$$\frac{d\hat{\sigma}_{WW ab}^{(\text{res.})}}{dM^2 dp_T^2}(p_T, M, \hat{s}; \alpha_S(\mu_R^2), \mu_R^2, \mu_F^2) = \frac{M^2}{\hat{s}} \int_0^\infty db \frac{b}{2} J_0(bp_T) \mathcal{W}_{ab}^{WW}(b, M, \hat{s}; \alpha_S(\mu_R^2), \mu_R^2, \mu_F^2), \tag{2.2}$$

where $J_0(x)$ is the 0-order Bessel function, μ_R (μ_F) is the renormalization (factorization) scale and $\hat{s}$ is the partonic centre-of-mass energy. By taking the N-moments of $\mathcal{W}$ with respect to the variable $z = M^2/\hat{s}$ at fixed M the resummation structure of $\mathcal{W}_{ab,N}^F$ can indeed be organized in exponential form [1]

$$\mathcal{W}_N^{WW}(b, M; \alpha_S(\mu_R^2), \mu_R^2, \mu_F^2) = \mathcal{H}_N^{WW}\left(M, \alpha_S(\mu_R^2); M^2/\mu_R^2, M^2/\mu_F^2, M^2/Q^2\right)$$
$$\times \exp\{\mathcal{G}_N(\alpha_S(\mu_R^2), L; M^2/\mu_R^2, M^2/Q^2)\}, \tag{2.3}$$

were we have defined the logarithmic expansion parameter L as

$$L \equiv \ln \frac{Q^2 b^2}{b_0^2} \tag{2.4}$$

and the coefficient $b_0 = 2e^{-\gamma_E}$ ($\gamma_E = 0.5772\ldots$ is the Euler number) has a kinematical origin. The scale Q appearing in eqs. (2.3), (2.4), named resummation scale in ref. [26], parametrizes the arbitrariness in the resummation procedure, and has to be chosen of the order of the hard scale M. Variations of Q around M can give an idea of the size of yet uncalculated higher-order logarithmic contributions. The function $\mathcal{H}_N^{WW}$ does not depend on the impact parameter b and it includes all the perturbative terms that behave

---

[1]Here, to simplify the notation, flavour indices are understood, or in other words, we limit ourselves to discussing the flavour non-singlet contribution. A complete discussion of the exponentiation structure in the general case can be found in appendix A of ref. [26].

as constants as $b \to \infty$. It can thus be expanded in powers of $\alpha_S = \alpha_S(\mu_R^2)$:

$$\mathcal{H}_N^{WW}(M, \alpha_S; M^2/\mu_R^2, M^2/\mu_F^2, M^2/Q^2) =$$
$$= \sigma_{WW}^{(0)}(\alpha_S, M)\Big[1 + \frac{\alpha_S}{\pi}\mathcal{H}_N^{WW\,(1)}(M^2/\mu_R^2, M^2/\mu_F^2, M^2/Q^2)$$
$$+ \left(\frac{\alpha_S}{\pi}\right)^2 \mathcal{H}_N^{WW\,(2)}(M^2/\mu_R^2, M^2/\mu_F^2, M^2/Q^2) + \dots\Big] \quad (2.5)$$

where $\sigma_{WW}^{(0)}$ is the Born partonic cross section. The exponent $\mathcal{G}_N$ includes the complete dependence on b and, in particular, it contains all the terms that order-by-order in α_S are logarithmically divergent as $b \to \infty$. The logarithmic expansion of $\mathcal{G}_N$ reads

$$\mathcal{G}_N(\alpha_S(\mu_R^2), L; M^2/\mu_R^2, M^2/Q^2) = L g^{(1)}(\alpha_S L) + g_N^{(2)}(\alpha_S L; M^2/\mu_R^2, M^2/Q^2)$$
$$+ \frac{\alpha_S}{\pi}g_N^{(3)}(\alpha_S L, M^2/\mu_R^2, M^2/Q^2) + \dots \quad (2.6)$$

where the term $L\, g^{(1)}$ collects the LL contributions, the function $g_N^{(2)}$ includes the NLL contributions, $g_N^{(3)}$ controls the NNLL terms and so forth.

In the implementation of eq. (2.3) the resummation of the large logarithmic contributions affects not only the small-p_T region ($p_T \ll M$), but also the region of large p_T ($p_T \sim M$). This can be easily understood by observing that the logarithmic expansion parameter L is divergent as $b \to 0$. To reduce the impact of unjustified higher-order contributions in the large-p_T region, the logarithmic variable L in eq. (2.4) is replaced as

$$L \to \tilde{L} \qquad \tilde{L} \equiv \ln\left(\frac{Q^2 b^2}{b_0^2} + 1\right). \quad (2.7)$$

The variables L and $\tilde{L}$ are equivalent when $Qb \gg 1$, but they lead to a different behaviour of the form factor at small values of b (i.e. large values of p_T). When $Qb \ll 1$ in fact, $\tilde{L} \to 0$ and $\exp\{\mathcal{G}_N\} \to 1$. The replacement in eq. (2.7) has thus a twofold consequence: it reduces the impact of resummation at large values of p_T, and it allows us to recover the corresponding fixed-order cross section upon integration over p_T.

Another important property of the formalism of ref. [26] is that the process dependence (as well as the factorization scale and scheme dependence) is fully encoded in the hard function $\mathcal{H}^{WW}$. In other words, the functions $g^{(i)}$ are universal: they depend only on the channel in which the process occurs at Born level, ($q\bar{q}$ annihilation in the case of WW production). Their explicit expressions up to $i = 3$ are given in ref. [26] in terms of the universal perturbative coefficients $A_q^{(1)}$, $A_q^{(2)}$, $A_q^{(3)}$, $\tilde{B}_{q,N}^{(1)}$, $\tilde{B}_{q,N}^{(2)}$. In particular, the LL function $g^{(1)}$ depends on the coefficient $A_q^{(1)}$, the NLL function $g_N^{(2)}$ also depends on $A_q^{(2)}$ and $\tilde{B}_q^{(1)}$ and the NNLL function $g_N^{(3)}$ also depends on $A_q^{(3)}$ and $\tilde{B}_{q,N}^{(2)}$. All these coefficients are known except $A_q^{(3)}$. In our quantitative study (see section 3) we assume that the value of $A_q^{(3)}$ is the same as the one [30, 31] that appears in resummed calculations of soft-gluon contributions near partonic threshold.

We now turn to the hard coefficients $\mathcal{H}_{q\bar{q}\leftarrow ab,N}^{WW}$. The first order contributions $\mathcal{H}_{q\bar{q}\leftarrow ab,N}^{WW\,(1)}$ in eq. (2.5) are known. The flavour off-diagonal part is process independent and in the $\overline{\text{MS}}$

scheme it reads:

$$\mathcal{H}_{q\bar{q}\leftarrow gq,N}^{(1)} = \mathcal{H}_{gg\leftarrow qg,N}^{(1)} = \frac{1}{2(N+1)(N+2)} + \gamma_{qg,N}^{(1)} \ln \frac{Q^2}{\mu_F^2}\,, \qquad (2.8)$$

where $\gamma_{ab,N}^{(1)}$ are the LO anomalous dimensions. The flavour diagonal coefficient is instead process dependent, and, as shown in refs. [23, 24], it can be expressed in terms of the finite part $\mathcal{A}^{WW}$ [2] of the one-loop correction to the Born subprocess, computed in ref. [7]. We have [26]:

$$\mathcal{H}_{q\bar{q}\leftarrow q\bar{q},N}^{WW(1)} = C_F \left(\frac{1}{N(N+1)} + \frac{\pi^2}{6} \right) + \frac{1}{2}\mathcal{A}^{WW} - \left(B_q^{(1)} + \frac{1}{2}A_q^{(1)} \ln \frac{M^2}{Q^2} \right) \ln \frac{M^2}{Q^2} + 2\gamma_{qq}^{(1)} \ln \frac{Q^2}{\mu_F^2}\,.$$
$$(2.9)$$

The second order coefficients $\mathcal{H}_{q\bar{q}\leftarrow ab,N}^{WW(2)}$ in eq. (2.5) have not yet been computed.

We finally consider the finite component in eq. (2.1). This contribution has to be evaluated starting from the usual perturbative truncation of the partonic cross section and subtracting the expansion of the resummed part at the *same* perturbative order. This procedure allows us to combine the resummed and the finite component of the partonic cross section to achieve uniform theoretical accuracy over the entire range of transverse momenta. Note that, since for WW production at $p_T^{WW} \neq 0$ only the LO result is known ($WW+1$ parton), we can perform the matching at LO only.

In summary, the inclusion of the functions $g^{(1)}$, $g_N^{(2)}$ and of the coefficient $\mathcal{H}_N^{WW(1)}$ in the resummed component, together with the evaluation of the finite component at LO, allows us to perform the resummation at NLL+LO accuracy. The inclusion of the function $g_N^{(3)}$ (still performing the matching at LO) allows us to reach (almost) NNLL+LO accuracy [3]. The reason why we cannot claim full NNLL accuracy is that the NNLL contribution $\alpha_S g_N^{(3)}$ in the exponent in eq. (2.6) is of the same order of the terms coming from the combined effect of $\alpha_S^2 \mathcal{H}_N^{WW(2)}$ and $Lg^{(1)}$, which are not under control. For this reason, in the following section we will mainly rely on our NLL+LO prediction, regarding the NNLL+LO result as an indication of the size of NNLL effects.
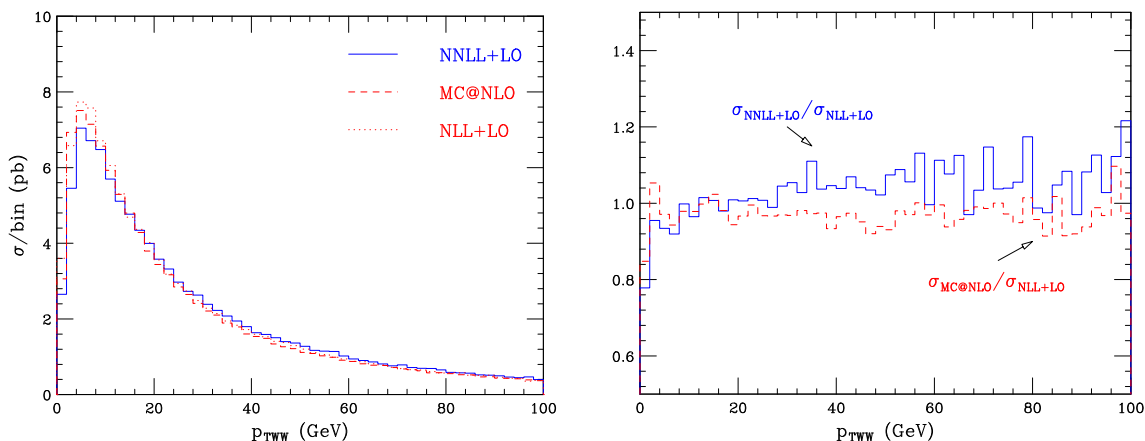
3. Results

In this section we present numerical results for WW production in pp collisions at LHC energies. We compare our resummed perturbative predictions at NLL+LO and NNLL+LO accuracy with the NLO ones, obtained with the general purpose program MCFM [9], and with results obtained with the MC@NLO event generator [28].

To compute the WW cross section we use MRST2002 NLO densities [32] and α_S evaluated at two-loop order. As discussed in section 2, our resummed predictions depend

---

[2]We adopt here for $\mathcal{A}^{WW}$ the definition of eq. (38) of ref. [24].

[3]The reader should not be confused by this notation: the NLL+LO and NNLL+LO results include the complete $\mathcal{O}(\alpha_S)$ real contribution through the finite component in eq. (2.1) as well as the full virtual $\mathcal{O}(\alpha_S)$ correction through the $\mathcal{H}_{q\bar{q}\leftarrow q\bar{q},N}^{WW(1)}$ coefficient in eq. (2.9). As a consequence, our NLL+LO and NNLL+LO results contain the complete NLO correction plus resummation of the large logarithmic contributions at $p_T^{WW} \ll M_{WW}$.

Figure 1: Left: comparison of the transverse momentum spectra of the WW pair obtained at NLL+LO, NNLL+LO and with MC@NLO. No cuts are applied. Right: NNLL+LO and MC@NLO results normalized to NLL+LO.

on renormalization, factorization and resummation scales. Unless stated otherwise, the resummation scale is set equal to the invariant mass M_{WW} of the WW pair, whereas renormalization and factorization scales are set to $2M_W$. The latter choice allows us to exploit our unitarity constraint and to exactly recover the total NLO cross section when no cuts are applied. At NLO we consistently use $\mu_F = \mu_R = 2M_W$ as default choice, whereas in MC@NLO μ_F and μ_R are set to the default choice, the average transverse mass of the W's.

The predictions of resummation are implemented in a partonic Monte Carlo program which generates the full 5-body final state ($l\nu l\nu$ + 1 parton). Nonetheless, since the resummed cross section in eq. (2.1) is inclusive over rapidity, we are not able to apply the usual rapidity cuts on the leptons[4]. To the purpose of the present work, we do not expect this limitation to be essential. Note also that, since the resummation formalism we use is valid for the inclusive production of a non-strongly interacting final state ($WW \to l\nu l\nu$ in the present case), we are not allowed to apply cuts on the accompanying jets.

We start by considering the inclusive cross sections. Our NLL+LO (NNLL+LO) result is 115.6 (115.5) pb, and agrees with the NLO one (116.0 pb) to better than 1%. The cross section from MC@NLO is instead lower, about 114.7 pb. The above difference is due to the different choice of the scales, and to the different convention in the choice of the electroweak couplings adopted in MC@NLO.

In figure 1 (left) we show the corresponding p_T distribution, computed at NLL+LO (dotted), NNLL+LO (solid) and with MC@NLO (dashed). The NLO result, not shown in the plot, diverges to $+\infty$ as $p_T^{WW} \to 0$. We see that the three histograms are very close to each other and show a peak around $p_T^{WW} \sim 5\,\mathrm{GeV}$. The agreement is confirmed in figure 1 (right) where the ratio of the NNLL+LO (solid) and MC@NLO (dashed) results to the NLL+LO are displayed. We see that, apart from statistical fluctuations, the MC@NLO and

---

[4]Note that this is not a limitation of principle: the resummation formalism can be extended to the double differential transverse momentum and rapidity distribution.
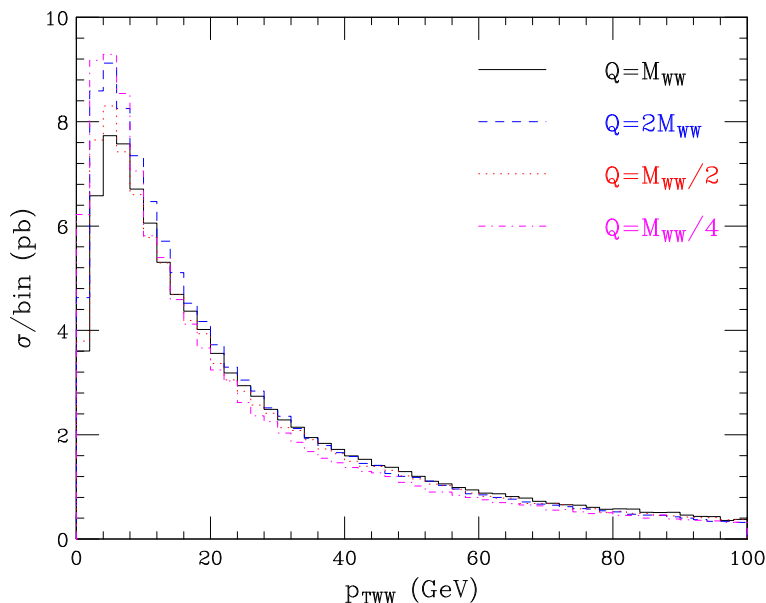
Figure 2: NLL+LO spectra for different values of the resummation scale Q.

NLL+LO agree within 2-3 % on average. On the contrary, the NNLL contribution tends to make the distribution harder and its effect increases at higher p_T, always being below 10%.

In order to study the perturbative uncertainties affecting our NLL+LO calculation, we have varied μ_F and μ_R by a factor 2 around the central value. We find that the effect of scale variations is rather small, of the order of $\pm 1\%$, and comparable with the estimated accuracy of our numerical code. Similar results are obtained by varying μ_F and μ_R in MC@NLO.

The dependence of our NLL+LO results on the resummation scale is instead stronger. In figure 2 we show the NLL+LO prediction for different values of the resummation scale Q. We see that varying the resummation scale the effect on the p_T^{WW} spectrum is well visible and amounts to about $\pm 10\%$ at the peak. For lower (higher) values of Q the effect of the resummation is confined to smaller (larger) values of p_T^{WW}. Comparing figures 1 and 2 we see that the order of magnitude of the NNLL effect, partially included in our NNLL+LO prediction, is smaller than the spread in the NLL+LO result from resummation-scale variations.

As in the case of Higgs production [26], we find that the choice $Q = 2M_{WW}$ gives (slightly) negative cross sections at very large p_T^{WW}. In order to define a range of variation of Q, we would like to avoid values that give a bad behaviour at large p_T^{WW}. For this reason in the following we will consider resummation-scale variations in the range $M_{WW}/4 \leq Q \leq M_{WW}$.

We now consider the p_T spectra of the leptons. For each event, we classify the transverse momenta of the two charged leptons into their minimum and maximum values, $p_{T\min}^l$ and $p_{T\max}^l$. In figure 3 we plot the corresponding p_T spectra, computed at NLL+LO (solid),
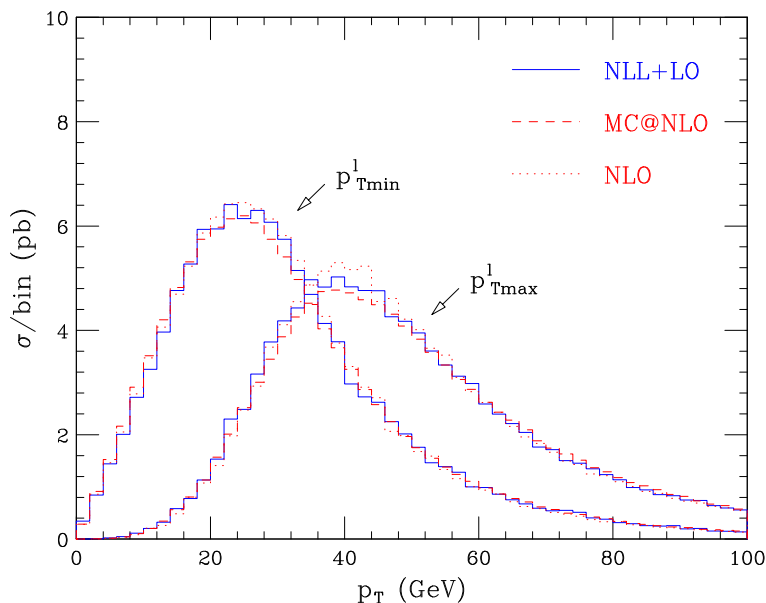
**Figure 3:** Distributions in $p^l_{T\min}$ and $p^l_{T\max}$. No cuts are applied.

NLO (dotted) and with MC@NLO (dashes). We see that all the three predictions are in good agreement. Small differences are visible in the peak of the p_T distribution of the lepton with larger p_T: the peak predicted by MC@NLO and by the NLL+LO calculation is slightly lower than the one from the NLO calculation. The renormalization- and factorization-scale dependence of the results, defined as above, is still of about $\pm 1\%$. The scale uncertainty of the NLL+LO result is dominated by resummation-scale variations and it is about $\pm 2 - 3\%$ on average.

We then examine the impact of resummation when cuts on the final state are applied. We start by defining the following selection criteria, taken from the study of ref. [29].

Cuts A:

- The p_T of the charged leptons should be larger than $20\,\mathrm{GeV}$.

- The invariant mass m_{ll} of the charged leptons should be smaller than $80\,\mathrm{GeV}$.

- The missing p_T of the event should be larger than $20\,\mathrm{GeV}$.

- The azimuthal separation $\Delta\phi$ of the charged leptons in the transverse plane should be smaller than 135°.

These cuts basically select a pair of W's, suppressing events with lepton pairs originating from the decay of a Z. The corresponding NLL+LO cross section is 21.03 pb, about 5% smaller than the NLO result of 22.10 pb. The MC@NLO cross section is instead 21.16 pb. The differences between these results are not unexpected: both the NLL+LO and the MC@NLO calculations enforce a unitarity constraint which ensure the correct NLO
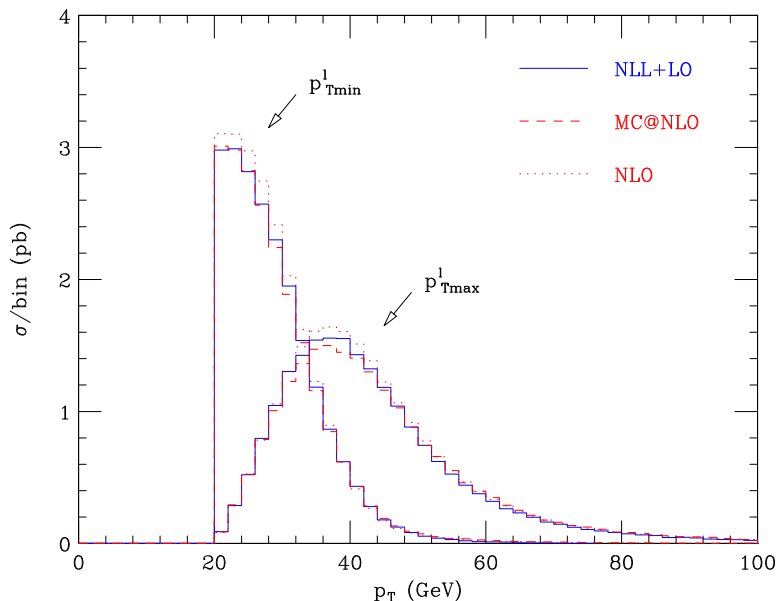
Figure 4: Distributions in $p^l_{T\min}$ and $p^l_{T\max}$. Cuts A are applied.

normalization is recovered when *total* cross sections are considered. When, as in this case, cuts are applied, higher order effects are present that make NLL+LO and MC@NLO results generally different from NLO.

In figure 4 we show the distributions in $p^l_{T\min}$ and $p^l_{T\max}$: as in figure 3, no significant differences are found between the three histograms: these distributions are still reliably predicted by the fixed-order NLO calculation. This conclusion is confirmed by studying scale variations. The effect of renormalization- and factorization-scale variations is still very small, and the impact of resummation-scale variations on the NLL+LO result is again of about $\pm 2 - 3\%$ on average.

In the search for the Higgs boson in the $H \to WW \to l\nu l\nu$ channel an important difference between the signal and the background is found in the $\Delta\phi$ distribution. Since the Higgs is a scalar, the charged leptons tend to be produced quite close in angle. As a consequence, the signal is expected to be peaked at small values of $\Delta\phi$, whereas the $\Delta\phi$ distribution for the background is expected to be reasonably flat. It is thus important to study the effect of resummation on this distribution, which is also known to be particularly sensitive to spin correlations [33].

In figure 5 the $\Delta\phi$ distribution at NLL+LO (solid) is compared to the one at NLO (dotted) and from MC@NLO (dashes). The upper panel shows NLL+LO and MC@NLO results normalized to the NLO prediction. Note that both the NLO and the NLL+LO calculations fully include spin correlations, whereas MC@NLO neglects spin correlations in the finite (non factorized) part of the one-loop contribution. We see that the agreement between the three results is excellent, showing that the approximate treatment of spin correlations in MC@NLO is accurate enough. Comparing NLL+LO and MC@NLO
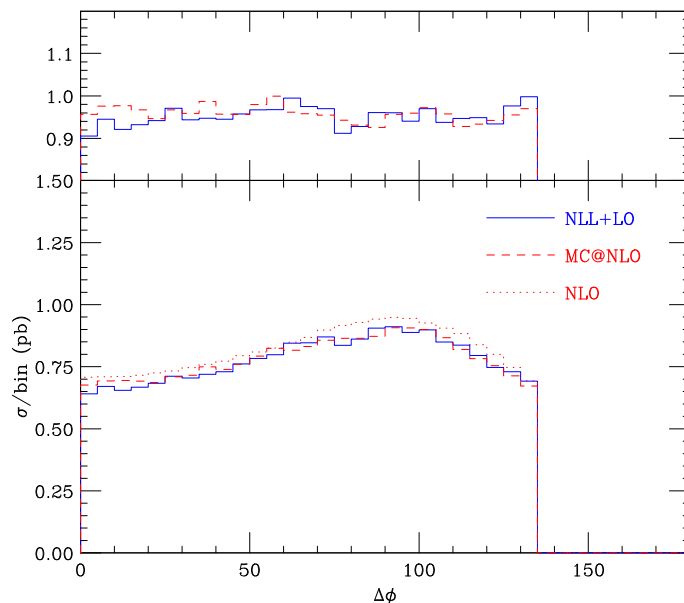
Figure 5: The $\Delta\phi$ distribution when cuts A are applied. The upper part of the plot shows the NLL+LO and MC@NLO results normalized to the NLO one.

predictions with NLO ones we also see that the effects of resummation appear negligible in this situation. As in the case of figure 4, this conclusion is confirmed by studying scale variations. The effect of renormalization- and factorization-scale variations is still of about $\pm 1\%$. The effect of resummation-scale variations on the NLL+LO prediction, not shown in the plot, is about $\pm 2\%$.

We now consider the application of stronger selection criteria [29], designed for the search of a Higgs boson with mass $M_H = 165\,\mathrm{GeV}$.

Cuts B

- For each event, $p^l_{T\mathrm{min}}$ should be larger than $25\,\mathrm{GeV}$ and $p^l_{T\mathrm{max}}$ should be between 35 and $50\,\mathrm{GeV}$.

- The invariant mass m_{ll} of the charged leptons should be smaller than $35\,\mathrm{GeV}$.

- The missing p_T of the event should be larger than $20\,\mathrm{GeV}$.

- The azimuthal separation $\Delta\phi$ of the charged leptons in the transverse plane should be smaller than 45°.

- A jet veto is mimicked by imposing that the transverse momentum of the WW pair should be smaller than $30\,\mathrm{GeV}$. This cut is perfectly legitimate in our resummed calculation and is exactly equivalent to a jet veto at NLO.

These cuts further select the small $\Delta\phi$ region. The jet veto is usually applied in order to reduce the $t\bar{t}$ contribution, which is expected to produce large-p_T b-jets from the decay of the top quark.
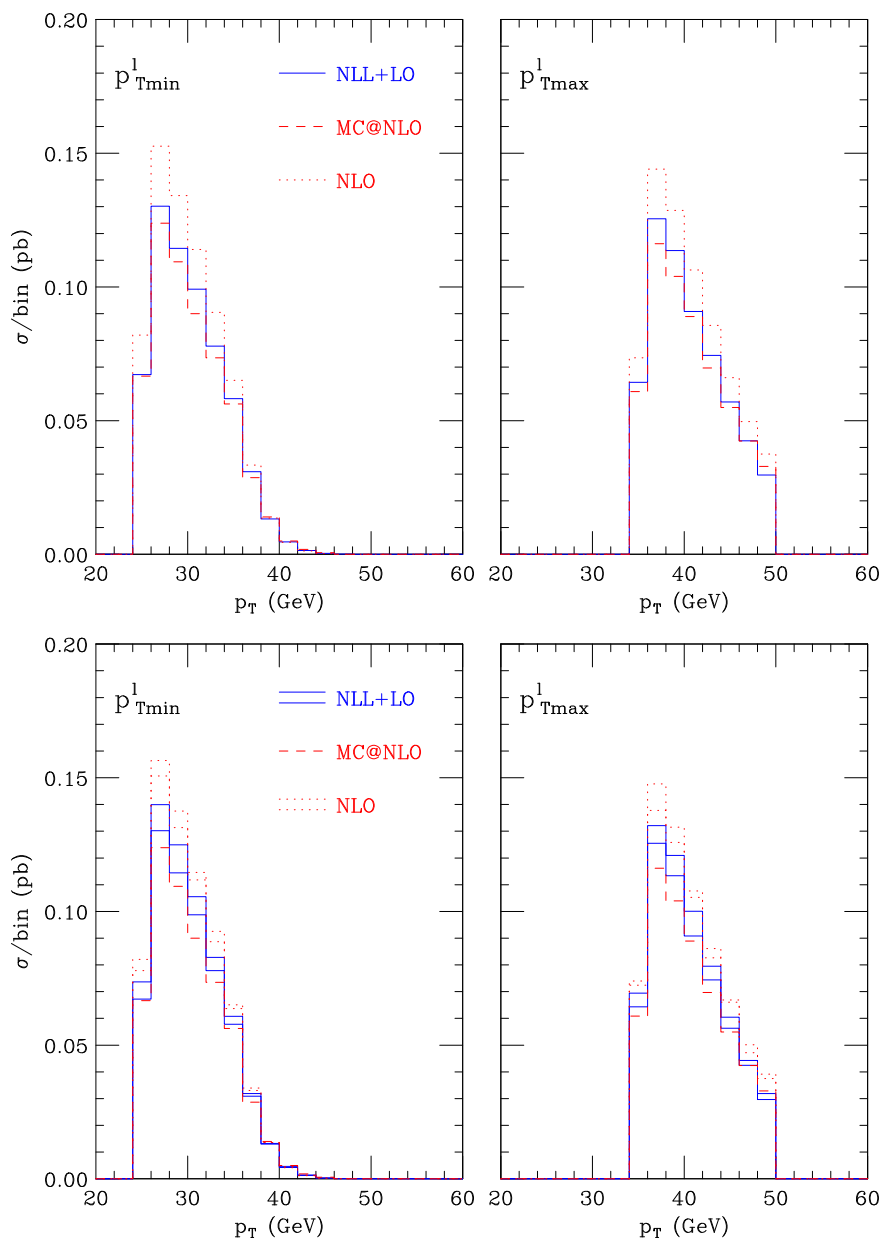
Figure 6: Distributions in $p^l_{T\min}$ and $p^l_{T\max}$ when cuts B are applied. In the lower plot the perturbative uncertainty bands at NLO and NLL+LO are shown.

The new cuts reduce the number of WW events by an additional factor of 35 with respect to cuts A. The NLL+LO (MC@NLO) accepted cross section is 0.599 pb (0.570 pb) which should be contrasted with the NLO result, which is 0.691 pb, about 20% higher. This relative large difference is due to the fact that the new cuts enhance the relevance of the small-p^{WW}_T region, where the NLO calculation is not any more reliable.

In figure 6 the $p^l_{T\min}$ and $p^l_{T\max}$ distributions are presented. The upper plot shows the two spectra for central values of the scales. We see that although the three predictions are
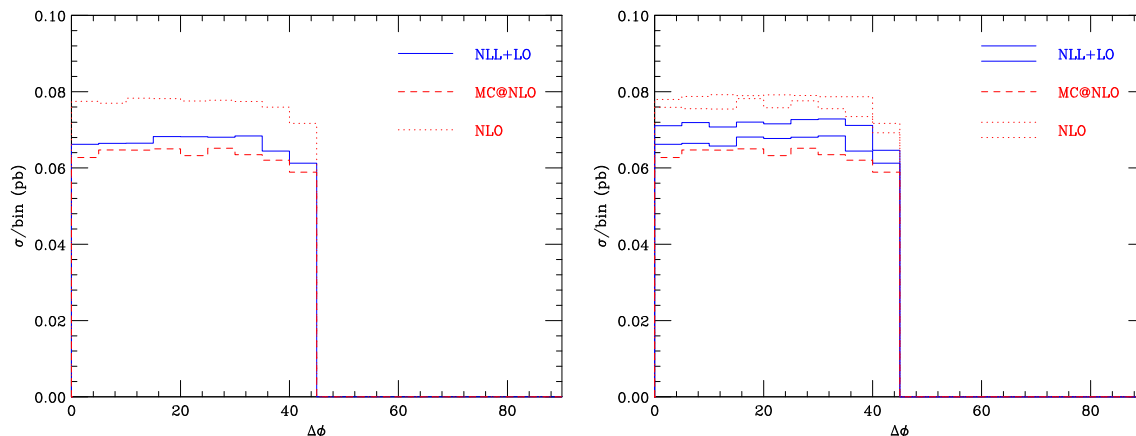
Figure 7: Left: $\Delta\phi$ distribution when cuts B are applied. Right: the corresponding NLL+LO and NLO uncertainty bands are shown.

still in reasonable agreement in shape, differences are now evident. In particular, the $p^l_{T\min}$ distribution at NLO is definitely steeper than the other two. Comparing NLL+LO and MC@NLO spectra, we see that the former are steeper than the latter: with the application of stronger cuts the differences between NLL+LO and MC@NLO predictions are clearly amplified. The lower plot shows the uncertainty band at NLO and NLL+LO. At NLO the band is obtained by varying $\mu_F = \mu_R$ between M_W and $4M_W$: the effect of scale variations is now more visible and is of the order of a few percent. The corresponding scale variations have marginal effect on the NLL+LO and MC@NLO results: this means that when the small p_T^{WW} region is selected, scale uncertainties increase at fixed order, while remaining small when resummation is included. At NLL+LO the band is obtained as before by varying the resummation scale Q between M_{WW} and $4M_{WW}$, and the effect is of about $\pm 3 - 4\%$.

In figure 7 (left) the $\Delta\phi$ distribution is displayed. The NLO and NLL+LO bands (right), computed as in figure 6, are also shown. We see that the shapes of the three results are still in good agreement with each other, although a slightly different slope of the NLL+LO result with respect to MC@NLO and NLO ones starts to appear.

We finally consider the transverse-mass distribution of the WW system. We choose to define the transverse mass according to ref. [34]. We start from the transverse energy of the charged leptons and of the neutrinos, which are expressed as

$$E_{Tll} = \sqrt{p_{Tll}^2 + m_{ll}^2} \qquad \displaystyle{\not}E_T = \sqrt{\displaystyle{\not}p_T^2 + m_{\nu\nu}^2}\,, \tag{3.1}$$

where $\mathbf{p}_{Tll}$ and $\displaystyle{\not}\mathbf{p}_T$ are the total transverse momentum of the charged leptons and the missing transverse momentum, respectively. If the Higgs boson mass is close to the WW threshold, the invariant mass of the neutrinos in the expression of $\displaystyle{\not}E_T$ can be approximated by m_{ll} and we can define

$$M_{TWW} = \sqrt{(\displaystyle{\not}E_T + E_{Tll})^2 - (\mathbf{p}_{Tll} + \displaystyle{\not}\mathbf{p}_T)^2}\,. \tag{3.2}$$
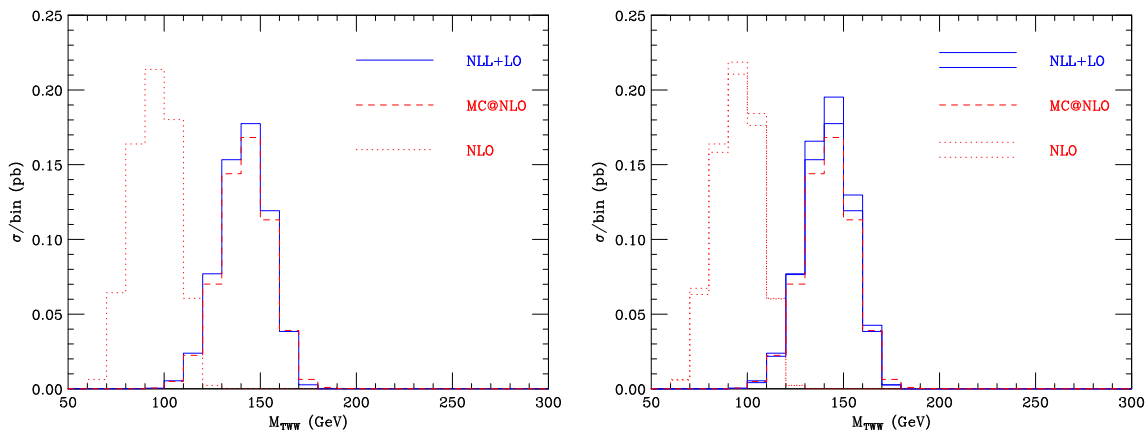
Figure 8: As in figure 7 but for the transverse-mass distribution.

In figure 8 we show the transverse-mass distribution defined above, computed at NLO (dotted), NLL+LO (solid) and with MC@NLO (dashes). The plot on the right shows the uncertainty bands computed as in figures 6, 7. We see that the effects of soft-gluon resummation are dramatic for this distribution: the NLL+LO result is shifted towards larger values of M_{TWW} by about $50\,\mathrm{GeV}$. We find that this big difference is mainly due to the leptonic cuts: removing the jet veto the shift in the transverse-mass distribution is basically unchanged. Comparing the shapes of the histograms we see that at NLO the shape is fairly different with respect to NLL+LO and MC@NLO. Also the NLL+LO and MC@NLO distributions now show clear differences: the position of the peak is the same but the NLL+LO result is steeper and softer than the MC@NLO one.

4. Summary

In this paper we studied the effects of soft-gluon resummation in WW pair production in hadron collisions. We performed a calculation that, using the helicity amplitudes computed in ref. [7], achieves uniform NLO accuracy over the whole phase space but consistently includes the resummation of the large logarithmic contributions at $p_T^{WW} \ll M_{WW}$. We presented predictions for the p_T^{WW} spectrum at NLL+LO and (almost) NNLL+LO accuracy, and compared our results with those obtained with the MC@NLO event generator, finding good agreement.

We then examined a few charged-lepton distributions: the p_T spectrum of the lepton with minimum and maximum p_T, the azimuthal separation of the charged leptons in the transverse plane and the transverse-mass distribution, when different sets of cuts are applied. The p_T spectra of the charged leptons are generally well described by the NLO calculation but the effect of resummation becomes visible when hard cuts are applied. The $\Delta\phi$ distribution is important to discriminate a Higgs-boson signal over the background in the $H \to WW \to l\nu l\nu$ channel, and is also known to be particularly sensitive to the effect of spin correlations in the W's decay. The latter are fully taken into account at NLO and in our NLL+LO calculation, whereas MC@NLO neglects spin correlations in the finite (non-

factorized) part of the one-loop contribution. All the predictions for the $\Delta\phi$ distribution agree well and resummation effects appear small even when hard cuts are applied.

The most striking effects are seen in the transverse mass distribution, whose prediction at NLO is very far from NLL+LO. On the other hand, the NLL+LO and MC@NLO results are still in reasonable agreement, although some differences appear in the shape of the distribution.

We finally note that the resummed predictions presented in this paper were obtained in a purely perturbative framework. Two kinds of non-perturbative effects may be considered: those due to hadronization, and those due to an intrinsic transverse momentum (intrinsic p_T) of the partons in the colliding hadrons.

In the present paper we were mainly concerned with leptonic observables. As a consequence, we do not expect hadronization effects to be particularly relevant. This expectation is supported by the good agreement we find between resummed results and MC@NLO predictions, in which hadronization effects *are* taken into account.

As far as intrinsic-p_T effects are concerned, it is known (see e.g. ref. [16] and references therein) that transverse-momentum distributions are affected by such kind of non-perturbative effects, particularly at small transverse momenta. These effects, associated to the large-b region in impact parameter, are not taken into account in our calculation. As noted in ref. [26], these non-perturbative effects have the same qualitative impact as the inclusion of higher-order logarithmic contributions, i.e., they tend to make the p_T distribution harder. The precise quantification of non-perturbative effects in WW production is left for future investigations.

Acknowledgments

References

[1] CDF and D0 collaborations, V.D. Elvira *Di-boson productions and SM SUSY Higgs searches at the Tevatron*, FERMILAB-CONF-05-329-CD, presented at *19th rencontres de physique de la Vallée d'Aoste: results and perspectives in particle physics*, La Thuile, Aosta Valley, Italy, 27 Feb - 5 Mar 2005.

[2] See e.g. J.F. Gunion, H.E. Haber, G.L. Kane and S. Dawson, *The Higgs hunter's guide*, Addison-Wesley, Reading, Mass. 1990.

[3] S.P. Martin, *A supersymmetry primer*, in *Perspectives in supersymmetry*, G.L. Kane ed., World Scientific, Singapore 1998 [`hep-ph/9709356`].

[4] M. Dittmar and H.K. Dreiner, *How to find a Higgs boson with a mass between 155 GeV to 180 GeV at the LHC*, Phys. Rev. **D 55** (1997) 167 [`hep-ph/9608317`].

[5] J. Ohnemus, *An order α_s calculation of hadronic W^-W^+ production*, *Phys. Rev.* **D 44** (1991) 1403.

[6] S. Frixione, *A next-to-leading order calculation of the cross-section for the production of W^+W^- pairs in hadronic collisions*, *Nucl. Phys.* **B 410** (1993) 280.

[7] L.J. Dixon, Z. Kunszt and A. Signer, *Helicity amplitudes for $\mathcal{O}(\alpha_s)$ production of W^+W^-, $W^\pm Z$, ZZ, $W^\pm\gamma$, or $Z\gamma$ pairs at hadron colliders*, *Nucl. Phys.* **B 531** (1998) 3 [hep-ph/9803250].

[8] L.J. Dixon, Z. Kunszt and A. Signer, *Vector boson pair production in hadronic collisions at $\mathcal{O}(\alpha_s)$: lepton correlations and anomalous couplings*, *Phys. Rev.* **D 60** (1999) 114037 [hep-ph/9907305].

[9] J.M. Campbell and R.K. Ellis, *An update on vector boson pair production at hadron colliders*, *Phys. Rev.* **D 60** (1999) 113006 [hep-ph/9905386].

[10] T. Binoth, M. Ciccolini, N. Kauer and M. Kramer, *Gluon-induced W W background to Higgs boson searches at the LHC*, *JHEP* **03** (2005) 065 [hep-ph/0503094].

[11] M. Duhrssen, K. Jakobs, J.J. van der Bij and P. Marquard, *The process $gg \to WW$ as a background to the Higgs signal at the LHC*, *JHEP* **05** (2005) 064 [hep-ph/0504006].

[12] Y.L. Dokshitzer, D. Diakonov and S.I. Troian, *Hard processes in quantum chromodynamics*, *Phys. Rept.* **58** (1980) 269.

[13] G. Parisi and R. Petronzio, *Small transverse momentum distributions in hard processes*, *Nucl. Phys.* **B 154** (1979) 427.

[14] G. Curci, M. Greco and Y. Srivastava, *QCD jets from coherent states*, *Nucl. Phys.* **B 159** (1979) 451.

[15] J.C. Collins and D.E. Soper, *Back-to-back jets in QCD*, *Nucl. Phys.* **B 193** (1981) 381, erratum *ibid.* **B 213** (1983) 545.

[16] J.C. Collins and D.E. Soper, *Back-to-back jets: Fourier transform from B to K-transverse*, *Nucl. Phys.* **B 197** (1982) 446.

[17] J. Kodaira and L. Trentadue, *Summing soft emission in QCD*, *Phys. Lett.* **B 112** (1982) 66; *Soft gluon effects in perturbative quantum chromodynamics*, report SLAC-PUB-2934 (1982); *Single logarithm effects in electron-positron annihilation*, *Phys. Lett.* **B 123** (1983) 335.

[18] G. Altarelli, R.K. Ellis, M. Greco and G. Martinelli, *Vector boson production at colliders: a theoretical reappraisal*, *Nucl. Phys.* **B 246** (1984) 12.

[19] J.C. Collins, D.E. Soper and G. Sterman, *Transverse momentum distribution in Drell-Yan pair and w and z boson production*, *Nucl. Phys.* **B 250** (1985) 199.

[20] S. Catani, D. de Florian and M. Grazzini, *Universality of non-leading logarithmic contributions in transverse momentum distributions*, *Nucl. Phys.* **B 596** (2001) 299 [hep-ph/0008184].

[21] C. Balazs, E.L. Berger, S. Mrenna and C.P. Yuan, *Photon pair production with soft gluon resummation in hadronic interactions*, *Phys. Rev.* **D 57** (1998) 6934 [hep-ph/9712471].

[22] C. Balazs and C.P. Yuan, *Higgs boson production at hadron colliders with soft gluon effects, I. Backgrounds*, *Phys. Rev.* **D 59** (1999) 114007 [hep-ph/9810319], erratum *ibid.* **D 63** (2001) 059902.

[23] D. de Florian and M. Grazzini, *Next-to-next-to-leading logarithmic corrections at small transverse momentum in hadronic collisions*, *Phys. Rev. Lett.* **85** (2000) 4678 [hep-ph/0008152].

[24] D. de Florian and M. Grazzini, *The structure of large logarithmic corrections at small transverse momentum in hadronic collisions*, *Nucl. Phys.* **B 616** (2001) 247 [hep-ph/0108273].

[25] G. Bozzi, S. Catani, D. de Florian and M. Grazzini, *The q_T spectrum of the Higgs boson at the LHC in QCD perturbation theory*, *Phys. Lett.* **B 564** (2003) 65 [hep-ph/0302104].

[26] G. Bozzi, S. Catani, D. de Florian and M. Grazzini, *Transverse-momentum resummation and the spectrum of the Higgs boson at the LHC*, hep-ph/0508068.

[27] S. Frixione and B.R. Webber, *Matching NLO QCD computations and parton shower simulations*, *JHEP* **06** (2002) 029 [hep-ph/0204244]; *Matching NLO QCD computations and parton shower simulations*, *JHEP* **06** (2002) 029 [hep-ph/0204244];
S. Frixione, P. Nason and B.R. Webber, *Matching NLO QCD and parton showers in heavy flavour production*, *JHEP* **08** (2003) 007 [hep-ph/0305252].

[28] S. Frixione and B.R. Webber, *The MC@NLO 3.1 event generator*, hep-ph/0506182.

[29] G. Davatz, G. Dissertori, M. Dittmar, M. Grazzini and F. Pauss, *Effective K-factors for $gg \to H \to WW \to \ell\nu\ell\nu$ at the LHC*, *JHEP* **05** (2004) 009 [hep-ph/0402218].

[30] A. Vogt, *Next-to-next-to-leading logarithmic threshold resummation for deep-inelastic scattering and the Drell-Yan process*, *Phys. Lett.* **B 497** (2001) 228 [hep-ph/0010146];
C.F. Berger, *Higher orders in $A(\alpha_s)/[1-x]_+$ of non-singlet partonic splitting functions*, *Phys. Rev.* **D 66** (2002) 116002 [hep-ph/0209107].

[31] S. Moch, J.A.M. Vermaseren and A. Vogt, *The three-loop splitting functions in QCD: the non-singlet case*, *Nucl. Phys.* **B 688** (2004) 101 [hep-ph/0403192];
A. Vogt, S. Moch and J.A.M. Vermaseren, *The three-loop splitting functions in QCD: the singlet case*, *Nucl. Phys.* **B 691** (2004) 129 [hep-ph/0404111].

[32] A.D. Martin, R.G. Roberts, W.J. Stirling and R.S. Thorne, *Uncertainties of predictions from parton distributions, I. Experimental errors*, *Eur. Phys. J.* **C 28** (2003) 455 [hep-ph/0211080].

[33] See e.g. T. Gleisberg, F. Krauss, A. Schalicke, S. Schumann and J.-C. Winter, *Studying W^+W^- production at the fermilab Tevatron with sherpa*, *Phys. Rev.* **D 72** (2005) 034028 [hep-ph/0504032].

[34] D.L. Rainwater and D. Zeppenfeld, *Observing $H \to W^{(*)}W^{(*)} \to e^{\pm}\mu^{\mp}\not{p}_t$ in weak boson fusion with dual forward jet tagging at the cern LHC*, *Phys. Rev.* **D 60** (1999) 113004 [hep-ph/9906218], erratum *ibid.* **D 61** (2000) 099901.

Erratum

The NLO results for the transverse mass distribution presented in figure 8 are not correct, due to a bug in the numerical calculation. The corrected plots are shown below.

The inset plot shows the NLO and MC@NLO results normalized to NLL+LO. The plot on the right shows the uncertainty bands computed as in figures 6, 7. All the three histograms are peaked at M_{TWW} between 140 and 150 GeV. Comparing the shapes of the histograms, we see that at NLO the shape is fairly different with respect to NLL+LO and MC@NLO. The NLL+LO and MC@NLO distributions also show small differences: the NLL+LO result is steeper and softer than the MC@NLO one.
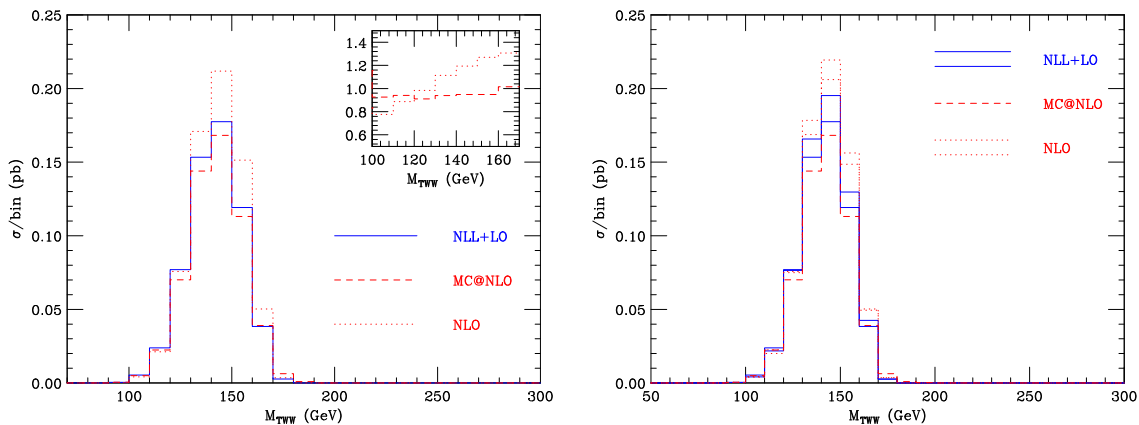
Figure 9: Left: M_{TWW} distribution when cuts B are applied. The inset plot shows NLO and MC@NLO results normalized to NLL+LO. Right: NLL+LO and NLO uncertainty bands computed as in figure 7